Thermophysics and Aeromechanics, 2015, Vol. 22, No. 5

Testing a dual-mode ramjet engine with kerosene combustion*

V.M. Levin[1], V.N. Karasev[1], L.L. Kartovitskii[1], E.A. Krymov[2], and O.A. Skachkov[2]

[1]*Moscow Aviation Institute (National Research University), Moscow, Russia*

[2]*Bardin Central Research Institute of Ferrous Metallurgy, Moscow, Russia*

E-mail: vadimlevin@yahoo.com

(*Received July 8, 2014; in revised form February 19, 2015*)

Results of life firing tests of a dual-mode ramjet engine intended for operation in the speed range M = 3–6 are discussed. The tests were carried out on a test bench under freestream conditions typical of Mach 6 flight at 27.6-km altitude. In the tests, the adopted design and technological solutions were verified, and efficient operation of the ramjet engine with kerosene combustion during 110 s was demonstrated.

Key words: dual-mode ramjet engine, kerosene, firing tests.

Ramjet-engine concept description, engine design, and problem statement

Activities aimed at the development of the wide-range ramjet engine concept were initiated at Moscow Aviation Institute in 1988 [1] by testing a dual-mode hydrogen combustion chamber with mechanically controlled flame holders [2]. The aviation-kerosene-fueled ramjet engine has been under design in 1998–2008 [3]. The engine was intended to power aircraft in the ranges of flight Mach number M_f = 3–6 and of flight altitude H_f = 0.5–30 km.

The ramjet engine of rectangular cross section comprised an air intake with duct-inlet dimensions 75×121 mm, a two-section combustor (with the two sections arranged in succession), and a supersonic nozzle with fixed throat whose cross-sectional dimensions were 70×85 mm. The total length of the engine, whose schematic is shown in Fig. 1, was 1985 mm.

In the model, a 3D wide-range mixed-compression air intake of original asymmetric design intended for the range of flight Mach number M_f = 3–6 was used. The external appearance of the engine is shown in Fig. 2. The air intake is rated for operation at M_f = 4. The design combustion initiation point is M_f = 2.95. The air intake has successfully passed gas-dynamic tests. In the range of Mach number M_f = 3–6, its characteristics vary in the following ranges: total pressure recovery coefficient is 0.62–0.25, flow rate coefficient is 0.7–0.98 (at zero angle of attack), mean Mach number in the throat is 1.6–2.9.

An original gas-dynamic arrangement of the two-section combustion chamber ensuring good performance characteristics of the combustor throughout the whole range of flight speeds was developed. As is seen in Fig. 1, the combustion chamber can be conventionally divided

* Dedicated to the memory of Eugeny Sergeevich Shchetinkov

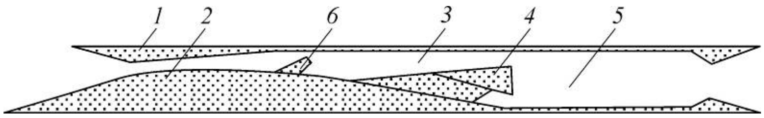

Fig. 1. Schematic of the dual-mode ramjet engine.
1 — air intake, *2* — insulator, *3* — upper section of combustion chamber, *4* — flame holder, *5* — lower section of combustion chamber, *6* — fuel supply assembly.

into two sections according to airflow motion, an upper section (*3*) and a lower section (*5*). The chamber can be operated in two modes with fuel burning adjustment and placement of the primary heat-release zone in one of the two sections depending on the flight speed. At flight Mach number $M_f = 3–5$, a subsonic burning regime is realized in the lower section, whereas at Mach number $M_f > 6$, a mode with fuel combustion in supersonic flow is realized in the upper section. The burning process in the combustion chamber is adjusted automatically depending on the value of air stagnation enthalpy at the inlet to the upper section of the chamber. Thus, whatever the particular value of excess air ratio, at air stagnation temperatures in excess of 1700 K the fuel ignition and burning processes proceed in the upper section according to the kinetic laws. In such an explicitly separated form, dual-mode operation has been implemented and demonstrated for the first time. Below we consider this operation mode in more detail.

During ignition, nitrogen-bubbled kerosene was supplied through two collectors normally to the carrier airflow from a two-row array of 2-mm thick planar struts of 36-mm height (two struts in each row). The first (along the flow) collector was intended for implementing small kerosene supplies, and the second collector was intended for implementing large kerosene supplies corresponding to low flight Mach numbers.

In the ramjet-engine design, a set of heat-resistant aviation materials meeting all requirements for efficient operation of the engine in the given range of ramjet-body aerodynamic-heating temperatures at maximum-speed flight under stoichiometric operating conditions of combustor (ultimate heating) was used. The materials must ensure high values of structural strength and erosion resistance. First of all, such materials included PKh25Yu6 powder alloy (developed at Bardin Central Research Institute of Ferrous Metallurgy). That material was used to fabricate the air inlet and the flame-holder strut. The flame holder, installed at the center of the chamber, was a vertical powder-alloy strut, whose end-face part prepared from a composite material was fixed on the strut from the side of the recirculation mixing zone. VKNA-V intermetallide was used to fabricate the fuel supply assembly (manufactured by Chernyshev Moscow Machine-Building Enterprise). The combustion chamber, the nozzle, and part of the flame holder were fabricated (at Central Research Institute for Special Machinery) of the UKM-15 carbon-carbon (CC) composite material covered with a special composite antioxidant coating. The problem of fabricating a ramjet shell of rectangular cross section of the CC composite material was solved in Russia for the first time. The installation of the ramjet engine on the testing bench is illustrated by Fig. 3.

In the tests, the following two main problems were solved. The first task was to implement steady operation of the air intake and combustion chamber at stoichiometric fuel supply and high process efficiency. The second task was to verify the design and technological solutions that were adopted while developing the engine.

Fig. 2. External appearance of the 3D air intake.

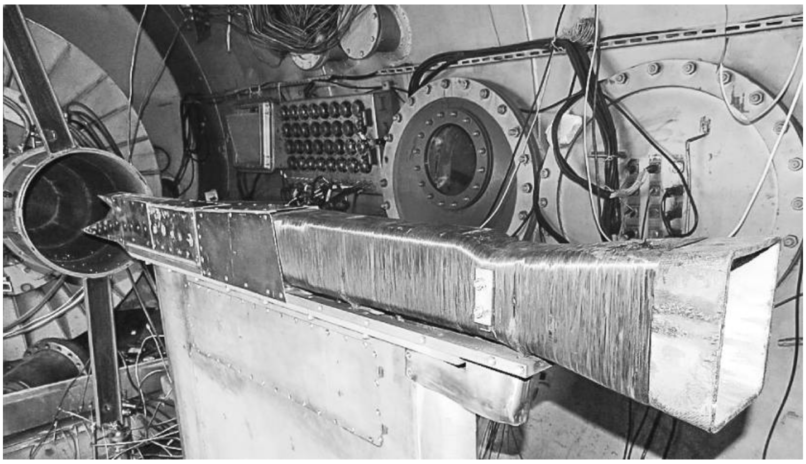

Fig. 3. Installation of the engine on the testing bench.

For performing the experiments, the following initial conditions were adopted:

– parameters of the airflow discharged from the heater nozzle: Mach number M_{Nh} = 6, stagnation pressure P_{Sh} = 27 bar, stagnation temperature T_{Sh} = 1662 K;

– engine setting angle equals 3°,

– basic measurement system: registration of all engine-start parameters, IR imaging (measurement of engine casing temperature during engine runs), thrust measurements, video-registration of both the engine in operation and the exhaust gas-jet flow.

Characteristics of the implemented burning process were obtained by the method of 1D through-calculations made along the engine flow duct with allowance for the variation of the thermophysical properties of air and combustion products, and with regard for the total pressure loss data that were previously obtained in tests of the two-section combustor with attached airline under conditions that modeled aircraft flights at M_f = 3, 4, 5, and 6 (see [3]). In the experiments, the engine thrust was determined by the weighing method as the change of the total drag force of the model in the flow with fuel burning. In the tests, only the axial force was taken into account. The analysis of testing data was performed by treating registered data on the parameters of engine runs with regard for the results of the visual control of engine behavior during engine starts, including air-intake operation, engine-shell heating, and the appearance of the discharged jet.

Testing results

In all engine runs, kerosene and a small amount of nitrogen necessary for bubbling the main fuel with the aim of promoting the firing process and reaching a stable operation of combustor were supplied through the first, low-discharge collector. To ensure thermal protection of the leading edge of fuel-injector struts, in bringing the air heater to normal operation, the nitrogen supply was affected prior to kerosene supply. In short runs, supply of hydrogen through the second collector and into the wake zone behind the flame holder was implemented. This was made for promoting or initiation of main-fuel ignition (since it was known from the previously gained experience that no self-ignition of kerosene was guaranteed in supersonic flow at air temperatures below 1700 K). To refine both the regime characteristics of the testing bench and the experimental procedure itself, two short technological runs of the experimental facility were performed prior to implementing the main life-test run.

The longitudinal diagram of pressure in the combustion chamber for various fuel expenditures is shown in Fig. 4. The graph in Fig. 4 and Table 1 give summarized results of the two short-duration runs and the long-duration run; here, α is the excess air ratio, the subscript

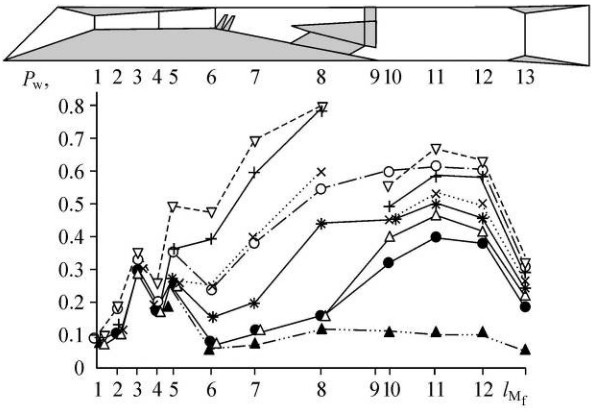

Fig. 4. Distribution of static pressure P_w over the ramjet-assembly flow-duct length l_{Mf} in the tests. Summary parameters are in Table 1.

Table 1

Signs	α_Σ	η	$\bar{R}$	Comments
▲	∞	–	–	Cold mode
●	2.5	–	–	Hydrogen supply into the 2nd collector
Δ	2.0	–	0.22	Hydrogen supply into the flame holder
Δ	1.0	–	–	Hydrogen and kerosene are supplied. No ignition
*	1.73	0.94	0.3	Kerosene burning
×	1.57	0.96	0.48	Kerosene burning
+	0.92	0.98	0.78	Kerosene burning
∇	0.95	–	0.91	Kerosene burning. Flame-holder strut has burnt out
○	0.98	0.95	1.0	Kerosene burning. No flame holder

Σ denotes the net value of α, η is the fuel combustion efficiency, and $\bar{R}$ is the ratio of the current thrust value to the maximum thrust that was registered in the regime with $\alpha_\Sigma = 0.98$. Pressure measurement stations (points 1–13) are shown at the lower wall of the engine. The discontinuity in the pressure curves between the eighth and tenth measurements is due to the absence of measurement point 9. Point 10 is in the wake zone of the flame-holder strut; this circumstance explains the cause of the assumed 5–10-% lowering of measured pressure. The figure illustrates the cold mode operation that corresponds to a situation in which the heater has reached the rated operating conditions in the absence of fuel supply into the engine.

Table 2 gives the longitudinal coordinates of static-pressure sensors over the flow channel of the engine (see Fig. 4).

In the first short run, hydrogen was supplied into the second collector unless normal operation of the heater was attained. Hydrogen self-ignition occurred in the lower section of the chamber; this process was accompanied by an increase in static pressure. At the time the heater had come to normal operation, additional supply of hydrogen into the zone behind the flame holder (mass flow rate 1.3 g/s) was effected; this supply had led to the burning of the injected hydrogen in the lower chamber and to an additional increase in pressure ($\alpha_{H_2} \approx 2$ in terms of the total hydrogen consumption). Under the latter conditions, kerosene supply with $\alpha_{ker} \approx 1$ induced no kerosene ignition. Termination of hydrogen supply into the second collector had not altered the situation. Subsequent, almost complete reduction of hydrogen supply into the wake zone behind the flame holder had not resulted in kerosene ignition either. Yet, at the moment the hydrogen supply was terminated with simultaneous reduction of kerosene supply to $\alpha_\Sigma = 1.73$, kerosene ignition, fast flame-crossing into the upper section, and an intense heating of this section had occurred. In the second short run, the situation had recurred at somewhat modified engine-starting procedure. Hydrogen supply only into the flame stabilization zone with $\alpha_\Sigma \approx 1.57$ had not led to kerosene ignition. Yet, on closing the hydrogen valve, with the rate of hydrogen flow being extremely small, kerosene had ignited in the lower section and, after a while, in the upper section, too.

Table 2

Location of static-pressure sensors

No.	Distance from the air-intake throat, mm
1	25
2	75
3	130
4	180
5	220
6	272
7	405
8	650
9	855
10	882
11	1040
12	1200
13	1258

Most likely, the results obtained in the two preliminary runs can be explained by realization of a certain value of excess air ratio α_Σ of the kerosene-hydrogen-air mixture in the recirculation mixing zone (in the wake behind the flame holder). The excess of the fuel in the pilot flame zone renders the combustor firing impossible.

An analysis of results of the technological runs has shown that the use of hydrogen under the conditions of interest is inexpedient. The kerosene burning process reliably sets in with no supply of hydrogen into the upper and/or lower section of the combustion chamber. The engine starting process without hydrogen supply was adopted in carrying out the main life test of the engine. The main run was performed without hydrogen yet with kerosene supply through the first collector at α_{ker} = 0.9–1. Kerosene self-ignition and pressure growth in the lower section of the combustion chamber had immediately resulted in the flame-crossing into the upper section with the combustion proceeding under conditions of a complex mixed and efficient (subsonic and supersonic) flow. Owing to the emergence of a pseudo-shock due to the initial ignition and, also, due to the kerosene firing in the lower section and thermal throttling, a specific phenomenon of kerosene firing in the upper section (in a supersonic flow) was realized.

A photo of the ramjet engine tested under conditions of long-duration life tests is shown in Fig. 5. Here, the heating of the combustion chamber at the 80th second of the testing procedure is shown.

Thus, the performed analysis of testing results for the ramjet engine with the chosen process arrangement under the adopted conditions has allowed the following conclusions to be made.

1. Hydrogen supply into the flame stabilization zone even in small amounts (α_{H_2} ~ 5–40) does not guarantee kerosene ignition in the lower section because of the overriching of the recirculation mixing zone with the fuel.

2. Kerosene self-ignition in the lower section of the combustion chamber provides for the formation of a steady fuel firing zone in the upper section, in the pseudo-shock that arises here due to the thermal throttling of the lower chamber. Intensification of the process is accompanied by a sharp increase in glow intensity of the gas flow at the nozzle exit. Under such conditions, approximately five-fold rise of pressure in the combustion chamber and a sharp reduction of engine aerodynamic drag (thrust) are observed, both observations providing confirmation for rather high an intensity of the heat-release process. In this way, normal operation of the engine is implemented.

The conclusion that the main heat-release zone was in the flow channel of the engine was made on the basis of the following results: (i) occurrence of an extended zone of strong heating of the engine shell in the region of the upper section (zone with the maximum shell temperature); such a zone would not occur in the absence of heat release in this region and (ii) no occurrence of flameout after flame-holder destruction and the preservation of elevated pressure.

The main life-test run was a step in the preliminary development cycle of the engine under conditions that modeled aircraft flight with Mach number $M_f = 6$ at 27.6-km altitude.

During the main run, the flame-holder strut had burnt out; the latter had led to the following result. After clearing of flow passage area, the burning process in supersonic flow continued, that is, the flame was not out. The latter had become the cause for the total reduction of static pressure in the combustor. Nonetheless, in the latter case, the engine thrust had increased by ≈ 10–15 %, presumably due to the reduction of the total pressure losses induced by the presence of a high-drag body in the channel.

Fig. 5. Firing of the ramjet engine during the life tests.

Discussion

In the experiments, normal operation of the ramjet engine corresponding to $M_f = 6$ with kerosene combustion with $\alpha = 1$ in the upper section of combustion chamber was implemented. The total run time of the engine, including the two preliminary runs of the combustor with the total duration of 20 seconds, was 110 seconds. The operation of the air intake was found stable with respect to pressure variations in the combustor.

In our experiments, a high kerosene combustion efficiency of $\eta = 0.94–0.98$ was attained. The combustion efficiency factor was calculated by 1D procedure from the distribution of static pressure in the channel of specified geometry. The maximum rise of shell-surface temperature to 1200 °C was found to occur in the zone of the upper section of the combustor. The air-intake geometry had remained unchanged, — both the clean smooth leading edges and the initial (i.e., linear) shape were retained. During the tests, no damages or material erosion markings were detected on the inner surfaces of the chamber and nozzle channel. The shell of the combustor has preserved its shape, with only a small amount of the binder forming the external taping of the carbon-filled plastic shell having been identified on the external surface. In the fuel supply assembly, no changes of the injector-structure shape had been noticed. In the flame holder, the following process took place: after the supersonic burning regime in the upper chamber set in, the stream temperature ahead of the flame holder (rated value 2650 K) proved to be 930 degrees higher than the rated working temperature of PKh25Yu6 alloy. At the 35th second, melting of the metal strut of the flame holder and material entrainment into the incoming stream has begun. By the 55th second, the flame holder has become fully cut. After the stabilizer has burned out, the thrust has insignificantly increased (by ~ 15 %), with the engine nonetheless continuing its operation in scramjet mode.

Conclusions

The results of life firing tests of the dual-mode ramjet engine under freestream conditions of integrally 110-s duration that modeled aircraft flight at $M_f = 6$ and $H_f = 27.6$ km under full thermal load have demonstrated the following:

– the operation of the 3D air intake proved to be stable with respect to pressure variations in the combustor;

– the flow-duct shape of the engine with the two-section combustor proved capable of enabling reliable combustor firing implemented according to an original gas-dynamic scheme that necessitated no application of stimulators or fuel-igniting means as well as of ensuring efficient steady burning process in supersonic combustion mode at stoichiometric fuel input;

– proper choice and feasibility of normal operation of the following heat-resistant materials used in the fabrication of ramjet-engine-body structural elements were confirmed: PKh25Yu6 powder alloy (used for fabrication of the air intake), UKM-15 CC composite material covered with special composite anti-oxidant coating, VKNA-V intermetallide; no material defects or erosion were found to occur on the external and internal surfaces of the flow duct of the combustion chamber and nozzle;

– further study of the engine design seems to be expedient.

References

1. **V.M. Levin,** Gas-dynamic of flow structure in a channel under thermal and mechanical throttling, in: Proc. 1st Int. Symp. on Experimental and Computational Aerothermodynamics of Internal Flows (July 8–12, 1990), Beijing, China, 1990, P. 763–767.
2. **V.N. Avrashkov, S.V. Grigoriev, D.M. Davidenko, and V.M. Levin,** Methodology of the experimental studies of ramjet combustion chamber operation at Moscow Aviation Institute, in: Theory of Ramjet Engines and Their Components: Collection of Scientific Papers, V.I. Bakulev (editor), Moscow Aviation Institute, Moscow, 1995, P. 8–9.
3. **V.M. Levin,** Problems of implementing ramjet operation, Combustion, Explosion, and Shock Waves, 2010, Vol. 46, No. 4, P. 408–417.